

## TEM investigation of high-pressure reaction-sintered cBN-Al composites

XIAO-ZHENG RONG, T. YANO

Research Laboratory for Nuclear Reactors, Tokyo Institute of Technology, O-okayama, Meguro-ku, Tokyo 152-8550, Japan

E-mail: xzrong@yahoo.co.jp

E-mail: tyano@nr.titech.ac.jp

Cubic boron nitride (cBN) has high hardness and excellent thermal conductivity [1]. Cubic BN composites are generally used as cutting tools for many hardened steels. However, fabrication of cBN composites is very difficult, as a high-pressure and a high-temperature are required. Wentorf and Rocco [2] reported that aluminum alloy was added to assist sintering of cBN. Since then, applications of cBN composites have become more and more important. Hibbs and Wentorf [3] developed high cBN content cutting tools, which were infiltrated by molten Al-Co from WC-Co substrate into the cBN layer during high-pressure and high-temperature sintering. Recently, the present authors [4] also reported that cobalt infiltration into a mixed cBN and WC layer played an important role in the densification of cBN. To improve thermal stability of cBN cutting tools, an addition of  $TiN_x$  or TiN was found to be useful [5, 6]. We synthesized cBN-Al composites sintered at high-pressure and high-temperature, and measured the effect of the amount of Al and sintering temperature on the hardness of the composites, and it was found that reactions occurred between cBN and molten aluminum [7]. In this work, the microstructure of the cBN-Al composites sintered under high pressure was studied by means of transmission electron microscopy and energy dispersive spectrometry, and the reaction mechanism was investigated.

Average particle sizes of starting powders, cubic BN (SBN-F, Showa Denko, Japan), and aluminum (Rare Metallic, Japan) were about 2.0 and 3.0  $\mu\text{m}$ , respectively. Mixing composition of the starting materials ranged between 50 and 90 mol% cBN. The rest was aluminum. The mixed powders with different compositions were sintered under 5.8 GPa between 900 and 1400  $^{\circ}\text{C}$  for 30 min using a Link-type cubic anvil apparatus [8, 9] with a 10 mm anvil edge length. Experimental details have been described elsewhere [7].

Samples for TEM were ground on polishing cloths with 3.0 and 0.5  $\mu\text{m}$  diamond pastes to a thickness of approximately 100  $\mu\text{m}$  using a polishing machine (Model ML-150S, Maruto, Japan). Then the thin sample (4 mm in diameter) was cut into small pieces available for a TEM specimen holder. A hollow was made at the center of the plate by using a dimple grinder (Model 656N, GATAN, USA) with diamond paste. Thickness of the samples as measured at the center of the dimple was about 20  $\mu\text{m}$ . The dimpled sample was then mounted on a molybdenum grid, 3 mm in diameter, and further

thinned until perforation by argon-ion thinning, with a beam current of 0.2 mA per gun (ION TECH, England). The foils were examined using an H-9000 electron microscope (TEM, Hitachi, Japan), operating at 300 kV and equipped with an energy dispersive X-ray detector (EDX, Model Delta IV, Kevex, USA). The phase of each grain was determined by the analysis of diffraction patterns and EDX chemical analysis.

The phases in the sintered specimens detected by X-ray diffractometry (XRD) were as follows: From the 50 to 60 mol% cBN mixing composition specimens (hereafter "composition" means mixing composition), reaction compounds were AlN, AlB<sub>2</sub>, and  $\alpha$ -AlB<sub>12</sub>; from the 65 to 75 mol% cBN composition specimens, reaction compounds were AlN, AlB<sub>2</sub>; and from the 80 to 90 mol% cBN composition specimens, reaction compounds were AlN and  $\alpha$ -AlB<sub>12</sub>, after sintering for both 1200 and 1400  $^{\circ}\text{C}$ . However, as well as AlN and AlB<sub>2</sub>, metallic Al phase was also detected for the 90 mol% cBN composition specimen sintered at 900  $^{\circ}\text{C}$ . The result indicated that similar reactions occurred during sintering at 1200–1400  $^{\circ}\text{C}$  independent of composition. The local composition was not homogeneous, because AlB<sub>2</sub> and  $\alpha$ -AlB<sub>12</sub> did not appear systematically. Furthermore, the result indicated that  $\alpha$ -AlB<sub>12</sub> was at a high temperature stable phase even under pressure [10, 11]. We reported earlier that cBN reacted with aluminum [7]. Chemical reactions could not go to completion at low temperatures such as 900  $^{\circ}\text{C}$ , whereas reactions finished at higher temperatures such as 1200 and 1400  $^{\circ}\text{C}$ .

Fig. 1A is a dark-field transmission electron micrograph of the 90 mol% cBN specimen sintered under 5.8 GPa at 900  $^{\circ}\text{C}$  for 30 min. Fig. 1B and C show selected area diffraction (SAD) patterns of the areas marked by the arrows. The SAD patterns contained rings which corresponded to the diffraction spacings of aluminum. Size measurement of bright particles in Fig. 1A indicated that the grains of aluminum were less than 100 nm in diameter. These areas are believed to be a liquid phase at the sintering temperature of 900  $^{\circ}\text{C}$ , because grain size of the raw Al powder is much greater i.e., between 1.0 and 4.0  $\mu\text{m}$  [7], therefore liquid phase sintering at 900  $^{\circ}\text{C}$  in the cBN-Al system could be assumed. Presence of small aluminum grains indicated that the cooling rate was relatively high. In the area shown in Fig. 1A, a reaction between cBN and aluminum cannot be seen.

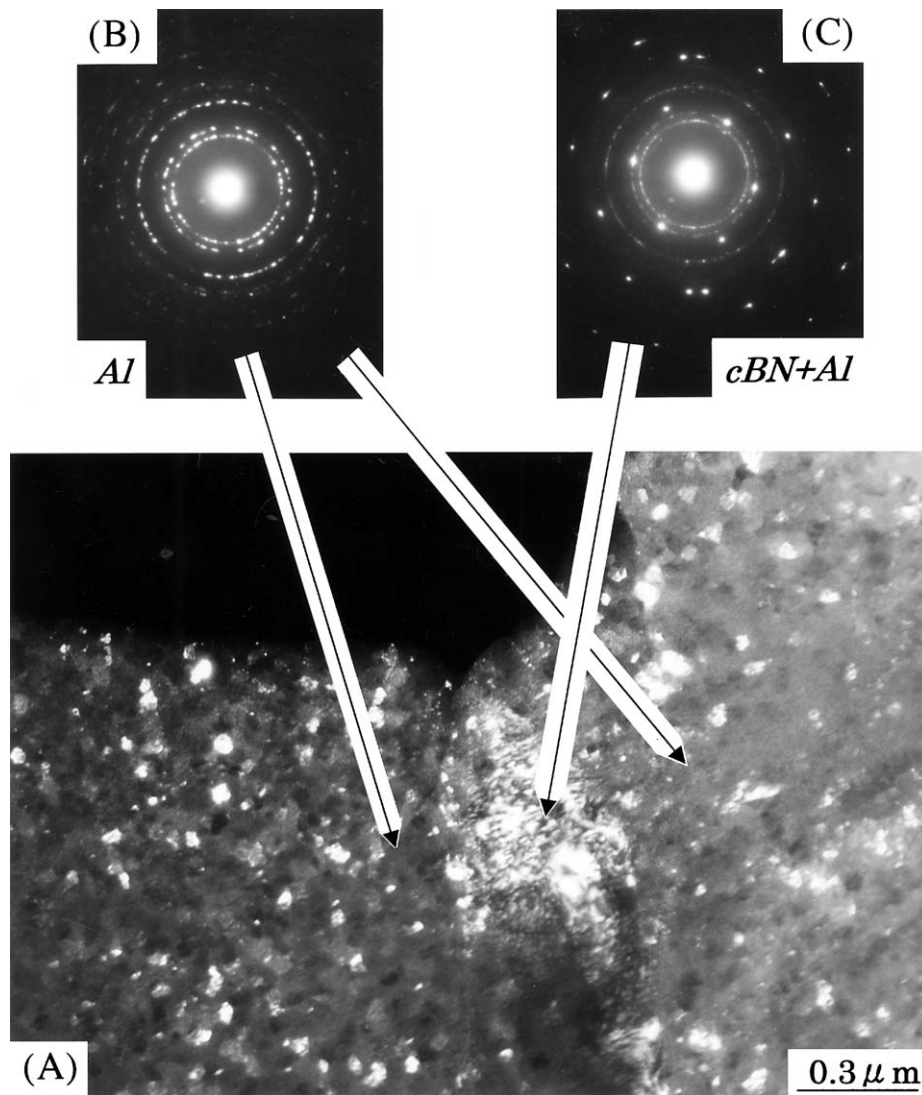


Figure 1 Transmission electron micrographs of the specimen containing 90 mol% cBN sintered under 5.8 GPa at 900 °C for 30 min: (A) Dark-field image, (B) SAD pattern of Al, (C) SAD pattern of cBN and Al.



Figure 2 Transmission electron micrograph of the specimen containing 90 mol% cBN sintered under 5.8 GPa at 900 °C for 30 min.

On the other hand, Fig. 2 shows a reacted area of the specimen containing 90 mol% cBN sintered under 5.8 GPa at 900 °C for 30 min. In Fig. 2, it can be seen that AlN grains are always found around cBN grains, shown with black arrowheads. We never found that AlB<sub>2</sub> grains existed next to cBN grains. That is to say, AlN grains always formed between cBN and AlB<sub>2</sub> grains. AlB<sub>2</sub> grains could grow to a large size of diameter of 2 μm. However, AlN existed as a polycrystalline layer. The arrow “O” shows that there is a sharp crack between two adjacent AlB<sub>2</sub> grains. Since these two AlB<sub>2</sub> grains showed the same crystallographic orientation, the crack was considered to have occurred inside a grain; AlB<sub>2</sub> has a graphite-like crystal structure and thus the inter-layer strength parallel to the basal plane should be very low. These cracks should affect the hardness of the specimen in the cBN-Al system.

The crack may be induced due to thermal stress during the cooling stage of the sintering process, because the thermal expansion coefficient of AlB<sub>2</sub> (graphite-like structure and no data about thermal expansion coefficient and anisotropy are available) is probably greater than those of AlN ( $\sim 4.5 \times 10^{-6}/\text{K}$ ) [12] or cBN ( $4.8\text{--}5.8 \times 10^{-6}/\text{K}$ ) [13].

Transmission electron micrograph of the specimen containing 65 mol% cBN sintered under 5.8 GPa at 1400 °C for 30 min is shown in Fig. 3. The reaction compound, AlN, always surrounds cBN grains, and AlB<sub>2</sub> grain always occurs next to AlN grains, as seen in Fig. 2. AlN appeared to be polycrystalline (variable contrast), whereas AlB<sub>2</sub> appeared as relatively large single grains (clear homogeneous contrast).

However, in Fig. 4A, we can see other area of the same specimen shown in Fig. 3. A large  $\alpha$ -AlB<sub>12</sub> grain

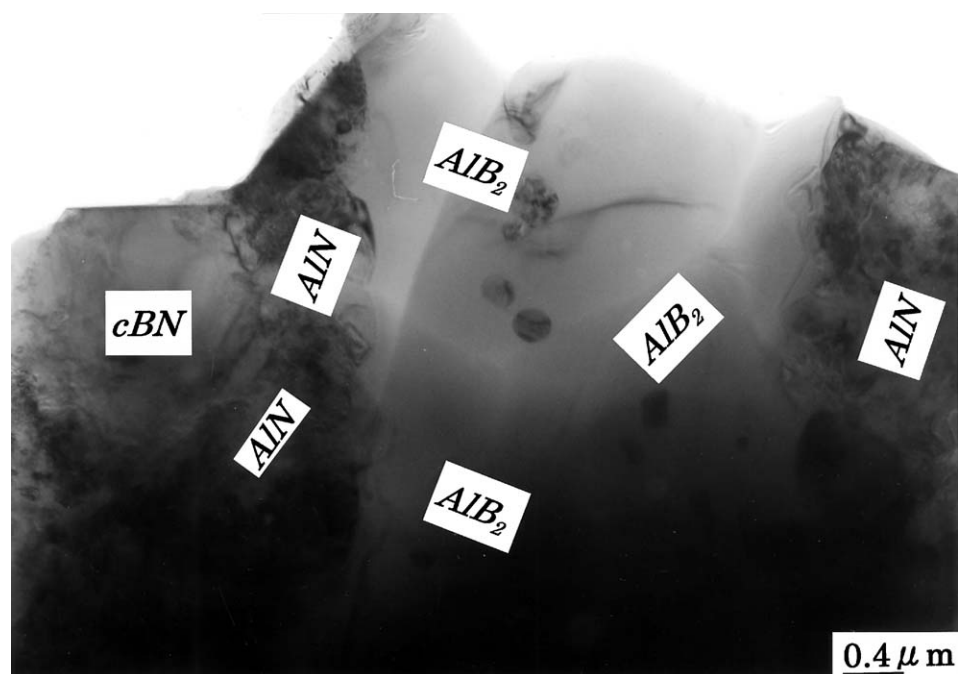


Figure 3 Transmission electron micrograph of the specimen containing 65 mol% cBN sintered under 5.8 GPa at 1400 °C for 30 min.

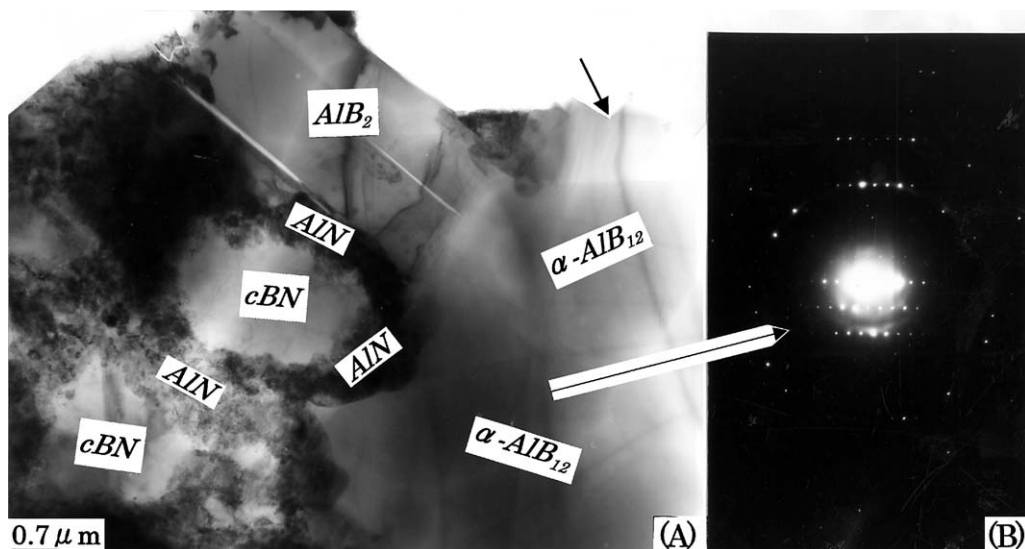


Figure 4 (A) Transmission electron micrograph of the specimen containing 65 mol% cBN sintered under 5.8 GPa at 1400 °C for 30 min, (B) SAD pattern of the grain shown by an arrow.



Figure 5 HREM micrograph of  $\alpha$ -AlB<sub>12</sub> grain marked by the arrow "C" in Fig. 4A.

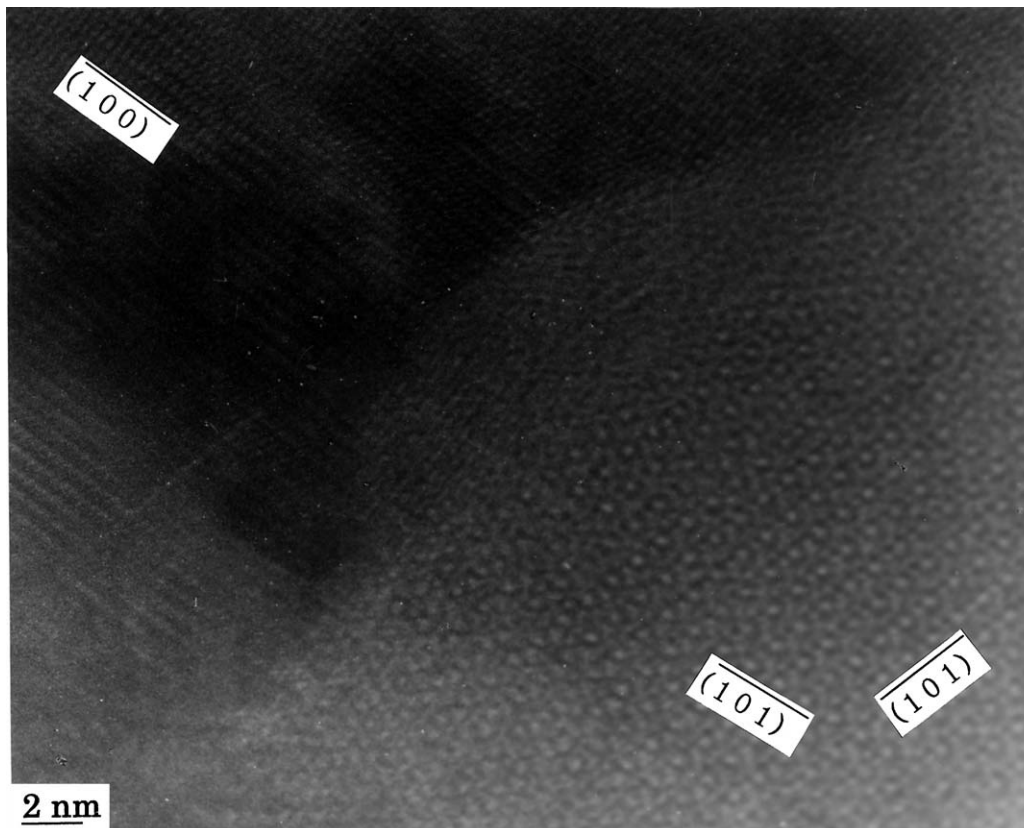


Figure 6 HREM micrograph of  $\alpha$ -AlB<sub>12</sub> (lower right) and AlB<sub>2</sub> crystal (upper left).

was confirmed by SAD pattern (Fig. 4B) and HREM image (Fig. 5), even though  $\alpha$ -AlB<sub>12</sub> could not be detected by XRD analysis in this composition. As found in Fig. 3, cBN grains were always surrounded by an AlN layer. The straight and sharp cracks between AlB<sub>2</sub> grains were observed as earlier shown in Fig. 2.

When using HREM imaging to investigate the 65 mol% cBN specimen sintered under 5.8 GPa at 1400 °C for 30 min, it was revealed that  $\alpha$ -AlB<sub>12</sub> grain

coexisted with AlB<sub>2</sub> grain, as shown in Fig. 6. At the same time, {111} twins were frequently observed in cBN grains, as shown in Fig. 7.

During the sintering, a melt of aluminum was formed and it reacted with cBN. The reaction did not proceed to completion at 900 °C. Above 1200 °C, metallic aluminum completely reacted with cBN. The reaction products such as AlN, AlB<sub>2</sub>, and  $\alpha$ -AlB<sub>12</sub> were formed independent of the composition of the cBN-Al system within the experimental compositional range



Figure 7 HREM micrograph of a twinned cBN crystal.

investigated. AlN was always found to be surrounding cBN grains as a polycrystalline layer. On the other hand,  $\text{AlB}_2$  and  $\text{AlB}_{12}$  were formed next to the AlN layer as relatively large grains. This indicates that the aluminum melt first fills the interstices between cBN grains. Reaction between cBN and Al occurs next. Al reacts at the surface of cBN grains to form a reaction product, AlN. As the reaction progresses, the reaction front moves into the cBN grains, resulting in an AlN, as observed in Figs 2–4. Whereas the crystal structure of cBN (zinc-blende type) and that of 2H-AlN (wurtzite type) are closely related, i.e., the structures resemble each other, no topotactic reaction occurred and large strain contrast was observed around cBN grains, probably due to the large difference in B-N interatomic distance (0.1567 nm) and Al-N interatomic distance (0.1885 nm). The molar volumes are also correspondingly significantly different ( $7.11 \text{ cm}^3/\text{mole}$  for cBN and  $12.54 \text{ cm}^3/\text{mole}$  for AlN). As a result of the reaction between BN and AlN, B should be released from BN. The B atoms are thought to diffuse through the AlN layer to reach unreacted metallic aluminum to form  $\text{AlB}_2$  or  $\text{AlB}_{12}$ . It is unclear at present why  $\text{AlB}_2$  or  $\text{AlB}_{12}$  were formed as relatively large single crystals, as observed in Figs 2–4. Formation of  $\text{AlB}_2$  or  $\text{AlB}_{12}$  grains in the composite should be restricted from the point of view of synthesizing hard materials, because these crystals show poor hardness and are easy to cleave, as shown in Figs 2 and 4. It is believed that the amount of cBN mainly controls the hardness of the composite i.e., a lower Al content and thus a higher amount of cBN results in higher hardness of the composites, as shown in a previous paper [7].

Since liquid aluminum has a lower viscosity at  $1400^\circ\text{C}$  than that at  $1200^\circ\text{C}$ , a better homogeneous microstructure was obtained after sintering at the higher temperature ( $1400^\circ\text{C}$ ). In other words, independent of cBN-Al composition, the hardness of the specimens sintered at  $1400^\circ\text{C}$  is higher than that at  $1200^\circ\text{C}$ , as mentioned in a previous work [7]. Another possibility for higher hardness of the  $1400^\circ\text{C}$ -sintered specimens is solid solution of B into AlN, resulting in the formation of small amounts of  $\text{AlB}_2$  or  $\text{AlB}_{12}$  in the composites. Evaporation of Al during heating process is also a possible reason.

### Acknowledgments

The authors appreciate Mr. M. Imai, of Research Laboratory for Nuclear Reactors, Tokyo Institute of Technology, for his support in the experiment.

### References

1. R. C. DE VRIES, in "Cubic Boron Nitride: Handbook of Properties," General Electric Tech. Rept. No. 72-CRD 178, (1972) Vol. 6, p. 968.
2. R. H. WENTORF JR., and W. A. ROCCO, Japanese Patent Appl. No. 65393 (1972).
3. L. E. HIBBS JR., and R. H. WENTORF JR., *HighTemp.-High Press.* **6**(4) (1974) 409.
4. X. Z. RONG and O. FUKUNAGA, *Diam. Films Tech.* **3**(2) (1993) 65.
5. A. HARA and S. YAZU, Japanese Patent Appl., 21633 (1979).
6. X. Z. RONG, T. TSURUMI, O. FUKUNAGA and T. YANO, *J. Diam. Rel. Mater.* **11** (2002) 280.
7. X. Z. RONG and O. FUKUNAGA, in "Advanced Materials 93, I/B", edited by M. Homma *et al.*, Trans. Mat. Res. Soc. Jpn. (Elsevier Science B.V., 1994) Vol. 14B, p. 1455.

8. M. WAKATSUKI, K. ICHINOSE and T. AOKI, *Jpn. J. Appl. Phys.* **10**(3) (1971) 357.
9. S. NAKANO, H. IKAWA and O. FUKUNAGA, *J. Amer. Ceram. Soc.* **75**(1) (1992) 240.
10. V. T. SEREBRYANSKII, V. A. EPELBAUM and G. S. ZHADANOV, *Dokl. Akad. Nauk SSSR*. **141**(4) (1961) 884; *Dokl. Chem. (Engl. Transl.)* **141**(4) (1961) 1244.
11. H. A. WRIEDT, *Bull. Alloy Phase Diagrams* **7**(4) (1986) 329, 395.
12. "Handbook of Ceramics," 2nd ed., edited by the Ceram Soc. Japan. (Gihodo Publishers, Tokyo, 2002) p. 122.
13. "Handbook of Ceramics," 2nd ed., edited by the Ceram Soc. Japan. (Gihodo Publishers, Tokyo, 2002) p. 120.

*Received 5 September 2003  
and accepted 8 March 2004*